Letter

Orbital order and superconductivity in bilayer nickelate compounds

Giniyat Khaliullin [1] and Jiří Chaloupka [2]

[1] *Max Planck Institute for Solid State Research, Heisenbergstrasse 1, D-70569 Stuttgart, Germany*

[2] *Department of Condensed Matter Physics, Faculty of Science, Masaryk University, Kotlářská 2, 61137 Brno, Czech Republic*

(Received 9 June 2025; revised 4 December 2025; accepted 2 January 2026; published 20 January 2026)

We propose a theory for bilayer nickelate materials, where a large tetragonal field—intrinsic or induced by epitaxial strain—lifts the orbital degeneracy and localizes the $3z^2-r^2$ orbital states. These states host local spins $S=1/2$ bound into singlets by strong interlayer coupling, and their dynamics is described by weakly dispersive singlet-triplet excitations ("triplons"). The charge carriers occupy the wide bands of x^2-y^2 symmetry, and their Cooper pairing is mediated by the high-energy triplon excitations. As the x^2-y^2 band filling increases, i.e., moving further away from the Ni^{3+} valence state, the indirect Ruderman-Kittel-Kasuya-Yosida interactions between local spins induce spin-density-wave order via triplon condensation. Implications of the model for compressively strained $La_3Ni_2O_7$ films and electron-doped oxychloride $Sr_3Ni_2O_5Cl_2$ are discussed.

DOI: 10.1103/4qsd-ws9c

Orbital degeneracy is a common feature of transition metal compounds and plays a fundamental role in a wide range of physical phenomena, from magnetism to metal-insulator and structural transitions [1–3]. In recent years, especially after the discovery of superconductivity (SC) in a number of nickel-based oxides [4–6], orbital physics has become a central issue also in the field of high-temperature superconductivity.

Nickelates are known for their rich spin, orbital, and electronic properties [1,7]. It is remarkable that the Ni valence states and spin-orbital structures in the nickelate SCs vary broadly. While $NdNiO_2$ [4] with Ni^+ ions and x^2-y^2 orbitals fits well into the cuprate's "single-layer, single-orbital, spin one-half" paradigm, $La_3Ni_2O_7$ [5,6] with mixed valence $Ni^{2.5+}$ ions is a bilayer system, and both x^2-y^2 and $3z^2-r^2$ orbitals are essential.

At ambient pressure, $La_3Ni_2O_7$ shows magnetic order, and becomes SC with $T_c\sim 80$ K under high pressure. Theoretical studies (see, e.g., [8–13] and references therein) suggest a strong pairing between the $3z^2-r^2$ electrons, while x^2-y^2 band is mostly responsible for the SC coherence within the planes. These theories are based on the multiorbital *ab-initio* band structures. The bilayer $t-J$ models were also considered, suggesting that SC is driven by an effective interlayer spin interaction between x^2-y^2 orbitals [14–16]. Experimentally, the key factors stabilizing SC in nickelates remain unclear, as the high-pressure conditions restrict the use of standard probes; significant local inhomogeneity in the structural and electronic properties [17,18] adds further uncertainties.

An important progress has been made recently: Under a compressive strain, the bilayer nickelate films exhibit SC even at ambient pressure [19–25]. Hole doping by oxidation or Sr doping is also essential. These observations raise fundamental questions about the microscopic origin of SC and its stabilization at ambient pressure, especially about the role played by the lattice strain.

Motivated by these observations, we propose in this Letter a theoretical model, which reveals a physical mechanism by which the in-plane compressive strain stabilizes the superconductivity in bilayer nickelates. The general phase behavior of the model, including magnetic ordering as a function of Ni valence, is discussed.

Our basic idea is that the compressive strain, which elongates the oxygen octahedra, lifts the e_g orbital degeneracy and localizes the $3z^2-r^2$ orbitals. The orbital ordering reduces the low-energy Hilbert space available for the charge carriers, thus promoting the metal-insulator Mott transition. As an illustration, let us consider a single-layer nickelate with Ni $d^7(t_{2g}^6e_g^1)$ configuration. The Mott transition takes place when Coulomb repulsion between electrons on different orbitals $U'=U-2J_{\rm H}$ ($J_{\rm H}$ is Hund's coupling) exceeds the e_g orbital bandwidth $W\sim 3-4$ eV. Due to pd-covalency, the effective interaction U' in nickelates is rather small, comparable to W, and they are typically metallic. In the presence of a tetragonal splitting Δ of the e_g level, however, the double occupation costs higher energy, $U'+\Delta$, which may well exceed W and thus stabilize the $3z^2-r^2$ orbital ordered Mott insulator. The case example is nickel oxyhalides Sr_2NiO_3X ($X=$ Cl, F), which are indeed antiferromagnetic Mott insulators [27], with an unpaired e_g electron in the $3z^2-r^2$ state.

The model. The basic structure of our model is shown in Fig. 1. The e_g level splitting $\Delta\sim 1$ eV, as evaluated in strained $La_3Ni_2O_7$ films [28,29] and oxychlorides [27,30] is assumed to be large enough to localize an electron in the $3z^2-r^2$ states, which overlap mainly on the interlayer c-axis bonds. The remaining e_g electrons, with an average density

Published by the American Physical Society under the terms of the Creative Commons Attribution 4.0 International license. Further distribution of this work must maintain attribution to the author(s) and the published article's title, journal citation, and DOI. Open access publication funded by Max Planck Society.

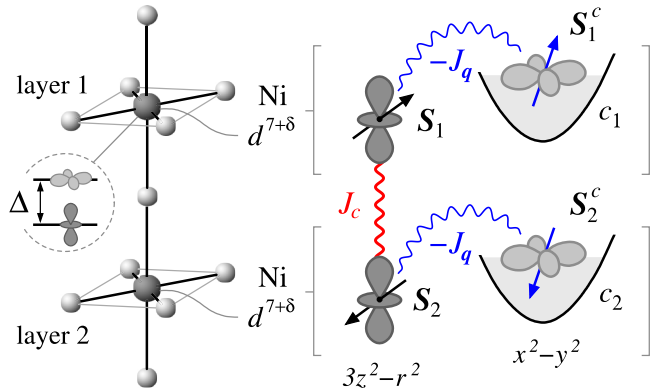


FIG. 1. Schematic of the model for a bilayer nickelate, where large e_g orbital splitting Δ (see inset) stabilizes the $3z^2-r^2$ states hosting local spins $\boldsymbol{S}_1$ and $\boldsymbol{S}_2$. The strong interlayer exchange coupling J_c (red wavy line) binds $\boldsymbol{S}_1$ and $\boldsymbol{S}_2$ into a singlet pair, forming a nonmagnetic background for the motion of the conduction electrons in the c_1 and c_2 bands of x^2-y^2 symmetry. The itinerant spins $\boldsymbol{S}_1^c$ and $\boldsymbol{S}_2^c$ couple to local spins by ferromagnetic interaction $-J_q$ (blue wavy lines).

$\delta < 1$ per Ni ion, occupy x^2-y^2 states forming wide conduction bands. The local and itinerant electrons interact via the Hund's and Kondo couplings. We now present the derivation of the model in detail.

(*i*) We start with the spin interactions between $3z^2-r^2$ orbitals. We use shorthand notations x and z for x^2-y^2 and $3z^2-r^2$ states, correspondingly, and parameterize their nearest-neighbor hoppings as follows. Strong overlap between z orbitals on the c-axis bonds gives the largest hopping denoted as $-t$, with $t>0$. The orbital hoppings on the nearest-neighbor in-plane bonds are then given by $t_{xx}=-\frac{3}{4}t$, $t_{zz}=-\frac{1}{4}t$, and $t_{xz}=\pm\frac{\sqrt{3}}{4}t$ (upper/lower sign corresponds to x/y bond direction) [31].

Standard calculations [2,33] give the following expressions for the interlayer J_c and intralayer J_{ab} exchange couplings between the local spins $\boldsymbol{S}$ hosted by z orbitals:

$$J_c=\frac{4t^2}{U},\quad J_{ab}/J_c=\frac{1}{16}\left(1-3\,\frac{J_{\rm H}}{U}\right). \tag{1}$$

The second term in J_{ab} is due to the interorbital t_{xz} hopping and Hund's coupling in a virtual state. With $t\simeq 0.6$ eV and $U\simeq 4.5$ eV, appropriate for Ni ions, we evaluate $J_c\simeq 0.3$ eV. Because of the weak overlap $t_{zz}/t=-1/4$ of z orbitals within the planes, J_{ab} is very small; a representative value of $J_{\rm H}\simeq 0.6$ eV gives $J_{ab}/J_c\simeq 0.04$. Thus, the local spins are tightly bound into interlayer singlet pairs of $\boldsymbol{S}_1$ and $\boldsymbol{S}_2$ (see Fig. 1). Following the bond-operator formalism for antiferromagnets [34,35], we define triplon $\boldsymbol{T}$ operators:

$$\boldsymbol{S}_{1,2}=\pm\frac{1}{2}(\boldsymbol{T}+\boldsymbol{T}^\dagger)-\frac{i}{2}(\boldsymbol{T}^\dagger\times\boldsymbol{T}), \tag{2}$$

where upper/lower sign refers to the first/second layer. Triplons are hard-core bosons describing singlet-triplet transitions within the c-axis dimer bonds. The exchange interactions on these bonds $J_c(\boldsymbol{S}_{i1}\cdot\boldsymbol{S}_{i2})$, and the in-plane interactions $J_{ab}(\boldsymbol{S}_{i1}\cdot\boldsymbol{S}_{j1}+\boldsymbol{S}_{i2}\cdot\boldsymbol{S}_{j2})$ on the nearest-neighbor bonds $\langle ij\rangle$

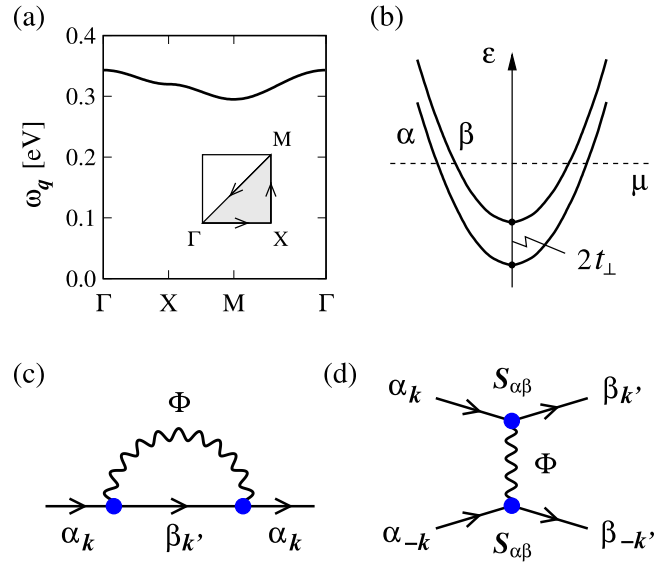


FIG. 2. (a) Momentum dependence of the singlet-triplet excitation energy $\omega_{\boldsymbol{q}}$, calculated with $t=0.6$ eV, $U=4.5$ eV, and $J_{\rm H}=0.6$ eV along $\Gamma(0,0)-{\rm X}(\pi,0)-{\rm M}(\pi,\pi)$ path. (b) Schematic of the bonding α and antibonding β band energies $\varepsilon_{\boldsymbol{k}}$ split by interlayer hopping $t_\perp$ [36]. The chemical potential μ is determined by the x^2-y^2 band filling δ. (c) Fermionic self-energy; the wavy line is the triplon propagator Φ describing singlet-triplet fluctuations, and the blue dots represent the spin exchange coupling $J_{\boldsymbol{k},\boldsymbol{k}'}$ between the local and itinerant electrons. (d) Pairing interaction mediated by the singlet-triplet fluctuations.

are expressed via $\boldsymbol{T}$ operators:

$$H_T=\sum_{\boldsymbol{q}}A_{\boldsymbol{q}}\boldsymbol{T}_{\boldsymbol{q}}^\dagger\boldsymbol{T}_{\boldsymbol{q}}+\frac{1}{2}\sum_{\boldsymbol{q}}B_{\boldsymbol{q}}(\boldsymbol{T}_{-\boldsymbol{q}}\boldsymbol{T}_{\boldsymbol{q}}+{\rm H.c.})+\ldots, \tag{3}$$

where $A_{\boldsymbol{q}}=J_c+2J_{ab}\gamma_{\boldsymbol{q}}$, $B_{\boldsymbol{q}}=2J_{ab}\gamma_{\boldsymbol{q}}$, and $\gamma_{\boldsymbol{q}}=(\cos q_x+\cos q_y)/2$. Far from magnetic order, triplon interactions, denoted by ellipsis in Eq. (3), and their hard-core nature can be neglected. The remaining quadratic form is diagonalized by the Bogoliubov transformation, leading to the triplon dispersion

$$\omega_{\boldsymbol{q}}=\sqrt{A_{\boldsymbol{q}}^2-B_{\boldsymbol{q}}^2}=J_c\sqrt{1+r\gamma_{\boldsymbol{q}}}, \tag{4}$$

where $r=4J_{ab}/J_c\ll 1$. As a result, local spin dynamics is described by weakly dispersive singlet-triplet excitations at high energies $\omega_{\boldsymbol{q}}\simeq J_c\simeq 0.3$ eV [see Fig. 2(a)].

(*ii*) Conduction electrons in the x^2-y^2 orbitals form wide bands, determined by large in-plane hopping $t_{xx}=-\frac{3}{4}t\sim -0.45$ eV, like in cuprates. Finite interlayer hoppings of the x^2-y^2 orbitals are allowed due to their virtual hoppings t_{xz} to $3z^2-r^2$ orbital levels and hybridization with the oxygen p states. These processes may operate within the c-axis rungs, $-t_\perp(c_{i1}^\dagger c_{i2}+{\rm H.c.})$, as well as connect the farther neighbors, $-t_\perp'(c_{i1}^\dagger c_{j2}+{\rm H.c.})$ with $j\neq i$. The main effect of these terms is to form bonding $\alpha_{\boldsymbol{k}}=\frac{1}{\sqrt{2}}(c_1+c_2)_{\boldsymbol{k}}$ and antibonding $\beta_{\boldsymbol{k}}=\frac{1}{\sqrt{2}}(c_1-c_2)_{\boldsymbol{k}}$ states with the dispersion relations

$$\varepsilon_{\boldsymbol{k}}^\alpha=-3t\gamma_{\boldsymbol{k}}-t_\perp,\quad \varepsilon_{\boldsymbol{k}}^\beta=-3t\gamma_{\boldsymbol{k}}+t_\perp, \tag{5}$$

which are depicted in Fig. 2(b). For simplicity, we omit here the long-range hoppings, which are present in real materials and modify the Fermi surface shapes [36], but not essential for our basic demonstration of the model.

(*iii*) Now we consider the interaction between local $\boldsymbol{S}$ and conduction electron spins $\boldsymbol{S}^c = \frac{1}{2} c^\dagger_{s'} \hat{\boldsymbol{\sigma}}_{s's} c_s$. There are two distinct spin exchange channels. First, the ferromagnetic Hund's coupling $-2J_{\rm H}(\boldsymbol{S}\cdot\boldsymbol{S}^c)$. Second, the antiferromagnetic Kondo interaction caused by virtual hoppings t_{xz} between nearest-neighbor z_i and x_j orbitals, $t_{xz}(x^\dagger_j z_i + z^\dagger_i x_j)$ with $t_{xz} = \pm\frac{\sqrt{3}}{4}t$. In $\boldsymbol{k}$-space, these processes lead to the following term in the Hamiltonian:

$$\sum_{\boldsymbol{k},\sigma} V_{\boldsymbol{k}} \sum_i e^{i\boldsymbol{k}\boldsymbol{R}_i} (c^\dagger_{\boldsymbol{k}\sigma} z_{i\sigma} + \text{H.c.}), \tag{6}$$

where $V_{\boldsymbol{k}} = \frac{\sqrt{3}}{2} t\, \eta_{\boldsymbol{k}}$ and $\eta_{\boldsymbol{k}} = (\cos k_x - \cos k_y)$. Treating this term perturbatively, we obtain the Kondo interaction:

$$H_{\rm K} = 2\sum_{\boldsymbol{k},\boldsymbol{k}'} V_{\boldsymbol{k}} V_{\boldsymbol{k}'} \left(\frac{1}{E^+} + \frac{1}{E^-}\right) (\boldsymbol{S}_{\boldsymbol{q}} \cdot \boldsymbol{S}^c_{\boldsymbol{k}',\boldsymbol{k}}), \tag{7}$$

where $\boldsymbol{S}^c_{\boldsymbol{k}',\boldsymbol{k}} = \frac{1}{2} c^\dagger_{\boldsymbol{k}'s'} \hat{\boldsymbol{\sigma}}_{s's} c_{\boldsymbol{k}s}$, and $\boldsymbol{k}' = \boldsymbol{k} + \boldsymbol{q}$. E^+ (E^-) is the energy cost required to add (remove) an electron to (from) a singly-occupied z orbital level.

The total interaction between the local and itinerant spins within a bilayer reads then as

$$H_{\rm int} = -\sum_{\boldsymbol{k},\boldsymbol{k}'} J_{\boldsymbol{k},\boldsymbol{k}'} \left[(\boldsymbol{S}_{\boldsymbol{q}} \cdot \boldsymbol{S}^c_{\boldsymbol{k}',\boldsymbol{k}})_1 + (\boldsymbol{S}_{\boldsymbol{q}} \cdot \boldsymbol{S}^c_{\boldsymbol{k}',\boldsymbol{k}})_2 \right], \tag{8}$$

where the coupling constant

$$J_{\boldsymbol{k},\boldsymbol{k}'} = 2J_{\rm H}(1 - \kappa\, \eta_{\boldsymbol{k}} \eta_{\boldsymbol{k}'}) \tag{9}$$

includes both Hund's and Kondo couplings. The latter brings about the momentum dependence in the exchange process, and its relative strength is given by

$$\kappa = \frac{3}{4}\frac{t^2}{J_{\rm H}\widetilde{E}}, \quad \text{where} \quad \frac{1}{\widetilde{E}} = \left(\frac{1}{E^+} + \frac{1}{E^-}\right). \tag{10}$$

The interorbital excitation energies E^+ and E^- depend on various parameters such as U, $J_{\rm H}$, intersite Coulomb interactions, tetragonal splitting, doping-dependent Fermi level position, etc. Using a representative value of $\widetilde{E} \simeq 1$ eV, and $t \simeq J_{\rm H} \simeq 0.6$ eV, we arrive at a rough estimate of $\kappa \simeq 0.5$. This implies that the overall coupling $J_{\boldsymbol{k},\boldsymbol{k}'}$ is ferromagnetic, and thus the model is free of the Kondo problem. We also note that, in contrast to manganites with large total spin $S = 2$, the Hund's splitting in nickelates is smaller than the e_g orbital bandwidth $W \sim 3 - 4$ eV, i.e., well below the double-exchange limit of $2J_{\rm H} > W$. For these reasons, we can safely treat the $J_{\boldsymbol{k},\boldsymbol{k}'}$ coupling (9) effects perturbatively. This is in contrast to the case of effective models (e.g. [14–16]) derived from a strong Hund's coupling limit of $J_{\rm H} \to \infty$.

Spin-singlet phase and superconductivity. We first rewrite Eq. (8) in terms of a triplon field defined as $\phi_\nu = \frac{1}{\sqrt{2}}(T + T^\dagger)_\nu \equiv \frac{1}{\sqrt{2}}(S_1 - S_2)_\nu$, where $\nu = (x, y, z)$. As the triplon density in the singlet phase is small, we keep ϕ-linear terms only:

$$H_{\rm int} = -\frac{1}{\sqrt{2}} \sum_{\boldsymbol{k},\boldsymbol{k}'} J_{\boldsymbol{k},\boldsymbol{k}'}\, \boldsymbol{\phi}_{\boldsymbol{q}} \cdot (\boldsymbol{S}_{\alpha\beta} + \boldsymbol{S}_{\beta\alpha})_{\boldsymbol{k}',\boldsymbol{k}}. \tag{11}$$

Here, spin density operator $(\boldsymbol{S}_{\alpha\beta})_{\boldsymbol{k}',\boldsymbol{k}} = \frac{1}{2}\alpha^\dagger_{\boldsymbol{k}'s'} \hat{\boldsymbol{\sigma}}_{s's} \beta_{\boldsymbol{k}s}$ connects bonding α and antibonding β fermions, as dictated by the odd parity of the triplon field.

Without magnetic order, the triplon Green's function matrix is diagonal and isotropic: $\Phi_{\nu\nu'} = \langle T_\tau \phi_\nu \phi_{\nu'} \rangle = \delta_{\nu\nu'}\Phi$. In harmonic approximation, i.e., neglecting triplon interactions, the bare Green's function is given by

$$\Phi_0 = \frac{J_c}{\omega^2 + J_c \Lambda_{\boldsymbol{q}}} \quad \text{with} \quad \Lambda_{\boldsymbol{q}} = J_c(1 + r\gamma_{\boldsymbol{q}}). \tag{12}$$

This propagator describes singlet-triplet excitations with the energy $\omega_{\boldsymbol{q}} = (J_c \Lambda_{\boldsymbol{q}})^{1/2}$ of Eq. (4). We use it to evaluate the fermionic self-energy in Fig. 2(c), and obtain the mass enhancement factor of $(1 + \lambda)$, where

$$\lambda \approx \frac{3}{2}\frac{J_{\rm H}^2}{J_c} N(0) \tag{13}$$

quantifies the coupling constant in the model. $N(0)$ is the density of states (per spin) at the Fermi level. We notice that λ has the same structure as in electron-phonon theories, with $J_{\rm H}$ and J_c playing the roles of electron-lattice coupling and phonon energy, respectively. As a rough estimate for λ, we may take $N(0) \simeq 0.2 - 0.3\ \text{eV}^{-1}$, $J_{\rm H} \simeq 0.6$ eV, $J_c \simeq 0.3$ eV, and obtain $\lambda \simeq 0.4 - 0.5$.

As in the electron-phonon problem, the same parameter λ quantifies the strength of the pairing interaction mediated by singlet-triplet excitations. Figure 2(d) shows that these excitations lead to the pair correlations between the bonding α and antibonding β states. We find that the SC order parameters on these bands have an opposite sign, $\Delta^{\rm SC}_\alpha = -\Delta^{\rm SC}_\beta$. This so-called $s_\pm$ symmetry is common to spin-mediated pairing models, including those proposed for nickelates [9,12]. However, the nature of the pairing glue in our theory, i.e., high-energy triplon excitations provided by the $3z^2 - r^2$ orbital sector, is radically different from the previous models. Observing the triplons would be the "smoking gun" for our theory.

BCS mean-field treatment of the interaction in Fig. 2(d) leads to high values of $T_c \sim \Omega \exp(-1/\lambda)$, where $\Omega = J_c$ (or Fermi energy ε_F at small doping δ), due to high excitation energy $J_c \sim 0.3$ eV and sizable coupling constant λ. Even though a more quantitative treatment of the model would reduce this estimate, it shows the great potential for high-T_c SC in the bilayer nickelates under a large tetragonal field.

Magnetic instability at large doping. We now consider the effects of the exchange coupling $J_{\boldsymbol{k},\boldsymbol{k}'}$ on local spins. Including this coupling, we obtain the Green's function Φ in the following form:

$$\Phi = \frac{J_c}{\omega^2 + J_c(\Lambda_{\boldsymbol{q}} + \Sigma_{\boldsymbol{q},\omega})}, \tag{14}$$

where the triplon self-energy $\Sigma_{\boldsymbol{q},\omega} = -4J_{\rm H}^2\, \widetilde{\chi}_{\boldsymbol{q},\omega}$ is determined by the $x^2 - y^2$ band spin susceptibility $\widetilde{\chi}_{\boldsymbol{q},\omega}$, see Fig. 3(a). Magnetic order, i.e., triplon condensation, takes place when the static ($\omega = 0$) self-energy obeys the equation $\Lambda_{\boldsymbol{q}} + \Sigma_{\boldsymbol{q}} = 0$. At a small density δ of the band electrons, their mutual interactions can be neglected, and $\Sigma_{\boldsymbol{q}}$ is given by the bare susceptibility $\chi_{\boldsymbol{q}}$, modified by the nonlocal nature of the

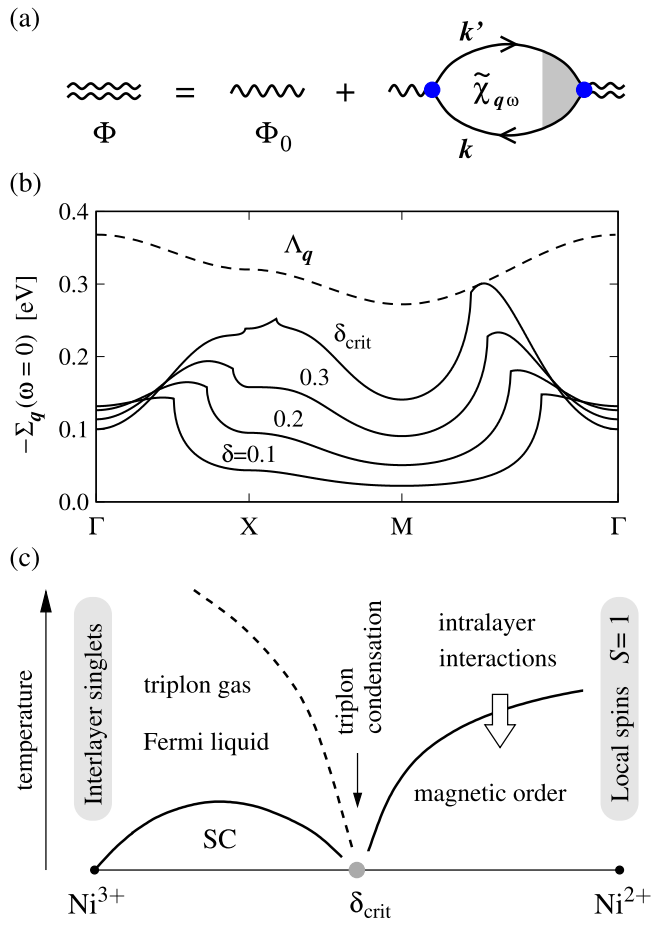


FIG. 3. (a) Triplon propagator Φ including the coupling $J_{k,k'}$ (blue dots) between the local and itinerant spins. The self-energy depends on the x^2-y^2 band spin susceptibility $\widetilde{\chi}_{q,\omega}$, enhanced by Hubbard correlations (shaded vertex) between conduction electrons. (b) The triplon self-energy at $\omega = 0$ for different dopings δ away from the Ni^{3+} valence state. At $\delta_{crit} \simeq 0.4$, the self-energy reaches the dashed curve Λ_q at some $\boldsymbol{q}$ between Γ and M points, and triplons condense into SDW order. Parameters used: $J_H = 0.6$ eV, $\kappa = 0.5$, and $t = 0.6$ eV. (c) Phase behavior of the $3z^2-r^2$ orbital-ordered bilayer nickelate as a function of Ni valence. Close to the Ni^{3+} end, the $3z^2-r^2$ local spins are bound into the interlayer singlet pairs, while the x^2-y^2 band electrons form a Fermi-liquid; singlet-triplet excitations (triplons) mediate their Cooper pairing. At large doping, $\delta > \delta_{crit}$, the intralayer RKKY interactions between local spins, mediated by the band electrons, induce magnetic order via triplon condensation.

exchange constant $J_{k,k'}$ (9):

$$\Sigma_q = -2J_H^2 \sum_k (1 - \kappa\, \eta_k \eta_{k'})^2\, \frac{n_k - n_{k'}}{\varepsilon_{k'} - \varepsilon_k}. \qquad (15)$$

The self-energy evolves quickly with doping, especially at momenta away from Γ point [see Fig. 3(b)], due to the Fermi surface shape and κ-term effects. As a result, the magnetic instability criteria are fulfilled already at $\delta \simeq 0.4$, i.e., well below the Mott limit for x^2-y^2 orbital sector. Physically, the magnetic order is driven by the indirect exchange interactions between local spins $\boldsymbol{S}$, mediated by the x^2-y^2 band electrons. Indeed, the triplon self-energy [a fermionic bubble in Fig. 3(a) and Eq. (15)] is nothing but the Ruderman-Kittel-Kasuya-Yosida (RKKY) interaction between local spins, and magnetic instability takes place when this interaction is large enough to overcome singlet-triplet gap $\Lambda_q \sim J_c$. There is a certain analogy with the Doniach's RKKY-vs-Kondo competition in heavy-fermion systems [37], though the origin of a nonmagnetic phase here (local spin dimers) is much different from Kondo singlet formation.

At the critical density δ_{crit}, a spin-density-wave (SDW) order sets in. Approaching half-filling of the x^2-y^2 band, $\delta = 1$, the enhanced Hubbard correlations are expected to cooperate with Hund's coupling, resulting in an antiferromagnetic Mott insulator with Ni^{2+} spins $S = 1$.

We sketch in Fig. 3(c) a global phase diagram of our model. Its core element is the interlayer spin-singlet dimers in the d^7 Mott insulator stabilized by orbital splitting. The superconductivity in the electron-doped spin-singlet phase is our main finding, which is a robust result based on the textbook treatment of a weakly interacting Fermi liquid coupled to the gapped singlet-triplet excitations. These excitations play the role of optical phonons in the BCS theory, and their high energy $\sim$0.3 eV and sizable coupling J_H to conduction spins should give rise to high-temperature superconductivity. The magnetic order at $\delta > \delta_{crit}$, resulting from competition between RKKY interactions and spin-singlet gap is also an intrinsic property of the model; however, its quantitative description is a nontrivial problem left for future work. From a broader perspective, it is important to extend the model for small Δ values, and clarify how its properties, especially superconductivity, evolve as the $3z^2-r^2$ electrons get delocalized to form a multiband metal.

On the materials side, the presence of a large tetragonal field is required to realize our model. We believe this is exactly the case of $La_3Ni_2O_7$ films under compressive strain [19–24]. Based on Fig. 3(c), it is also tempting to speculate that more hole doping of these nominally $\delta = 0.5$ materials may further increase the T_c values.

The recently synthesized oxychloride $Sr_3Ni_2O_5Cl_2$ [38] and similar mixed-anion compounds are also promising candidates. No ambient pressure transport data was reported for $Sr_3Ni_2O_5Cl_2$, but based on a theoretical prediction of large $\Delta \simeq 1$ eV [30], we expect it to be d^7 Mott insulator similar to Sr_2NiO_3X (X = Cl, F) [27]. Electron doping of this compound may lead to superconductivity.

To conclude, lifting the orbital degeneracy has profound implications for the electronic structure and superconductivity in bilayer nickelates. Large tetragonal field, be it intrinsic or induced by strain, stabilizes the cupratelike x^2-y^2 conduction band, which accommodates all the pairing strength generated by local spin fluctuations. The key difference from cuprates, however, is that the spin degrees of freedom in our model reside on a different ($3z^2-r^2$) orbital sector, and due to the bilayer structure, they form local singlets and are thus less harmful for the electron coherency in the x^2-y^2 band—a great advantage for superconductivity. This also offers a natural explanation for the recent observation of a Fermi-liquid behavior well above T_c in $La_2PrNi_2O_7$ films [23].

Acknowledgments. We thank M. Hepting and B. Keimer for useful discussions. G.K. acknowledges support from

the European Research Council under Advanced Grant No. 101141844 (SpecTera). J.C. acknowledges support by the Czech Science Foundation (GAČR) under Project No. GA22-28797S and by the project Quantum Materials for Applications in Sustainable Technologies, Grant No. CZ.02.01.01/00/22_008/0004572.

Data availability. The data that support the findings of this article are openly available [39].

[1] M. Imada, A. Fujimori, and Y. Tokura, Metal-insulator transitions, Rev. Mod. Phys. **70**, 1039 (1998).

[2] D. I. Khomskii, *Transition Metal Compounds* (Cambridge University Press, Cambridge, 2014).

[3] G. Khaliullin, Orbital order and fluctuations in Mott insulators, Prog. Theor. Phys. Suppl. **160**, 155 (2005).

[4] D. Li, K. Lee, B. Y. Wang, M. Osada, S. Crossley, H. R. Lee, Y. Cui, Y. Hikita, and H. Y. Hwang, Superconductivity in an infinite-layer nickelate, Nature (London) **572**, 624 (2019).

[5] H. Sun, M. Huo, X. Hu, J. Li, Z. Liu, Y. Han, L. Tang, Z. Mao, P. Yang, B. Wang, J. Cheng, D.-X. Yao, G.-M. Zhang, and M. Wang, Signatures of superconductivity near 80 K in a nickelate under high pressure, Nature (London) **621**, 493 (2023).

[6] G. Wang, N. N. Wang, X. L. Shen, J. Hou, L. Ma, L. F. Shi, Z. A. Ren, Y. D. Gu, H. M. Ma, P. T. Yang, Z. Y. Liu, H. Z. Guo, J. P. Sun, G. M. Zhang, S. Calder, J.-Q. Yan, B. S. Wang, Y. Uwatoko, and J.-G. Cheng, Pressure-induced superconductivity in polycrystalline $La_3Ni_2O_{7-\delta}$, Phys. Rev. X **14**, 011040 (2024).

[7] M. L. Medarde, Structural, magnetic, and electronic properties of $RNiO_3$ perovskites (R = rare earth), J. Phys.: Condens. Matter **9**, 1679 (1997).

[8] H. Sakakibara, N. Kitamine, M. Ochi, and K. Kuroki, Possible high-T_c superconductivity in $La_3Ni_2O_7$ under high pressure through manifestation of a nearly half-filled bilayer Hubbard model, Phys. Rev. Lett. **132**, 106002 (2024).

[9] Q.-G. Yang, D. Wang, and Q.-H. Wang, Possible $s_{\pm}$-wave superconductivity in $La_3Ni_2O_7$, Phys. Rev. B **108**, L140505 (2023).

[10] Z. Liao, L. Chen, G. Duan, Y. Wang, C. Liu, R. Yu, and Q. Si, Electron correlations and superconductivity in $La_3Ni_2O_7$ under pressure tuning, Phys. Rev. B **108**, 214522 (2023).

[11] Y.-F. Yang, G.-M. Zhang, and F.-C. Zhang, Interlayer valence bonds and two-component theory for high-T_c superconductivity of $La_3Ni_2O_7$ under pressure, Phys. Rev. B **108**, L201108 (2023).

[12] Y.-B. Liu, J.-W. Mei, F. Ye, W.-Q. Chen, and F. Yang, $s^{\pm}$-Wave pairing and the destructive role of apical-oxygen deficiencies in $La_3Ni_2O_7$ under pressure, Phys. Rev. Lett. **131**, 236002 (2023).

[13] F. Lechermann, J. Gondolf, S. Bötzel, and I. M. Eremin, Electronic correlations and superconducting instability in $La_3Ni_2O_7$ under high pressure, Phys. Rev. B **108**, L201121 (2023).

[14] H. Oh and Y.-H. Zhang, Type-II $t-J$ model and shared superexchange coupling from Hund's rule in superconducting $La_3Ni_2O_7$, Phys. Rev. B **108**, 174511 (2023).

[15] J. Chen, F. Yang, and W. Li, Orbital-selective superconductivity in the pressurized bilayer nickelate $La_3Ni_2O_7$: An infinite projected entangled-pair state study, Phys. Rev. B **110**, L041111 (2024).

[16] C. Lu, Z. Pan, F. Yang, and C. Wu, Interplay of two E_g orbitals in superconducting $La_3Ni_2O_7$ under pressure, Phys. Rev. B **110**, 094509 (2024).

[17] L. Liu, J. Guo, D. Hu, G. Yan, Y. Chen, L. Yu, M. Wang, X.-D. Liu, and X. Huang, Evidence for the Meissner effect in the nickelate superconductor $La_3Ni_2O_{7-\delta}$ single crystal using diamond quantum sensors, Phys. Rev. Lett. **135**, 096001 (2025).

[18] S. V. Mandyam, E. Wang, Z. Wang, B. Chen, N. C. Jayarama, A. Gupta, E. A. Riesel, V. I. Levitas, C. R. Laumann, and N. Y. Yao, Uncovering origins of heterogeneous superconductivity in $La_3Ni_2O_7$ using quantum sensors, arXiv:2510.02429.

[19] E. K. Ko, Y. Yu, Y. Liu, L. Bhatt, J. Li, V. Thampy, C.-T. Kuo, B. Y. Wang, Y. Lee, K. Lee, J.-S. Lee, B. H. Goodge, D. A. Muller, and H. Y. Hwang, Signatures of ambient pressure superconductivity in thin film $La_3Ni_2O_7$, Nature (London) **638**, 935 (2025).

[20] G. Zhou, W. Lv, H. Wang, Z. Nie, Y. Chen, Y. Li, H. Huang, W.-Q. Chen, Y.-J. Sun, Q.-K. Xue, and Z. Chen, Ambient-pressure superconductivity onset above 40 K in $(La,Pr)_3Ni_2O_7$ films, Nature (London) **640**, 641 (2025).

[21] Y. Liu, E. K. Ko, Y. Tarn, L. Bhatt, J. Li, V. Thampy, B. H. Goodge, D. A. Muller, S. Raghu, Y. Yu, and H. Y. Hwang, Superconductivity and normal-state transport in compressively strained $La_2PrNi_2O_7$ thin films, Nat. Mater. **24**, 1221 (2025).

[22] B. Hao, M. Wang, W. Sun, Y. Yang, Z. Mao, S. Yan, H. Sun, H. Zhang, L. Han, Z. Gu, J. Zhou, D. Ji, and Y. Nie, Superconductivity and phase diagram in Sr-doped $La_{3-x}Sr_xNi_2O_7$ thin films, arXiv:2505.12603.

[23] Y.-T. Hsu, Y. Liu, Y. Kohama, T. Kotte, V. Sharma, Y. Tarn, Y. Yu, and H. Y. Hwang, Fermi-liquid transport beyond the upper critical field in superconducting $La_2PrNi_2O_7$ thin films, arXiv:2505.19011.

[24] M. Osada, C. Terakura, A. Kikkawa, M. Nakajima, H.-Y. Chen, Y. Nomura, Y. Tokura, and A. Tsukazaki, Strain-tuning for superconductivity in $La_3Ni_2O_7$ thin films, Commun. Phys. **8**, 251 (2025).

[25] In $La_3Ni_2O_7$ films, the superconducting transition is broader and $T_c \sim 40$ K is lower than in the bulk, which can be attributed to the observed local inhomogeneities in lattice structure and oxygen stoichiometry [26].

[26] L. Bhatt, A. Y. Jiang, E. K. Ko, N. Schnitzer, G. A. Pan, D. F. Segedin, Y. Liu, Y. Yu, Y.-F. Zhao, E. A. Morales, C. M. Brooks, A. S. Botana, H. Y. Hwang, J. A. Mundy, D. A. Muller, and B. H. Goodge, Resolving structural origins for superconductivity in strain-engineered $La_3Ni_2O_7$ thin films, arXiv:2501.08204.

[27] Y. Tsujimoto, J. Sugiyama, M. Ochi, K. Kuroki, P. Manuel, D. D. Khalyavin, I. Umegaki, M. Månsson, D. Andreica, S. Hara, T. Sakurai, S. Okubo, H. Ohta, A. T. Boothroyd, and K. Yamaura, Impact of mixed anion ordered state on the magnetic ground states of $S = 1/2$ square-lattice quantum spin antiferromagnets, Sr_2NiO_3Cl and Sr_2NiO_3F, Phys. Rev. Mater. **6**, 114404 (2022).

[28] H. C. R. B. Bhatta, X. Zhang, Y. Zhong, and C. Jia, Structural and electronic evolution of bilayer nickelates under biaxial strain, arXiv:2502.01624.

[29] X.-W. Yi, W. Li, J.-Y. You, B. Gu, and G. Su, Unifying strain- and pressure-driven superconductivity in $La_3Ni_2O_7$: Suppressed charge and spin density waves and enhanced interlayer coupling, Phys. Rev. B **112**, L140504 (2025).

[30] M. Ochi, H. Sakakibara, H. Usui, and K. Kuroki, Theoretical study of the crystal structure of the bilayer nickel oxychloride $Sr_3Ni_2O_5Cl_2$ and analysis of possible unconventional superconductivity, Phys. Rev. B **111**, 064511 (2025).

[31] For simplicity, the Slater-Koster rules [32] are used; corrections due to non-cubic symmetry can be readily included, but they are not essential here.

[32] J. C. Slater and G. F. Koster, Simplified LCAO method for the periodic potential problem, Phys. Rev. **94**, 1498 (1954).

[33] A. M. Oleś, G. Khaliullin, P. Horsch, and L. F. Feiner, Fingerprints of spin-orbital physics in cubic Mott insulators: Magnetic exchange interactions and optical spectral weights, Phys. Rev. B **72**, 214431 (2005).

[34] S. Sachdev and R. N. Bhatt, Bond-operator representation of quantum spins: Mean-field theory of frustrated quantum Heisenberg antiferromagnets, Phys. Rev. B **41**, 9323 (1990).

[35] T. Sommer, M. Vojta, and K. W. Becker, Magnetic properties and spin waves of bilayer magnets in a uniform field, Eur. Phys. J. B **23**, 329 (2001).

[36] See Supplemental Material at http://link.aps.org/supplemental/10.1103/4qsd-ws9c for the long-range hopping effects on the band dispersions and Fermi surface shapes, which includes Refs. [40–42].

[37] S. Doniach, The Kondo lattice and weak antiferromagnetism, Physica B+C **91**, 231 (1977); See also P. Coleman, *Introduction to Many-Body Physics* (Cambridge University Press, Cambridge, 2015), Chap. 17.

[38] K. Yamane, Y. Matsushita, S. Adachi, T. Hiroto, R. Matsumoto, K. Terashima, H. Sakurai, and Y. Takano, High-pressure synthesis of bilayer nickelate $Sr_3Ni_2O_5Cl_2$ with a tetragonal crystal structure, Acta Cryst. C **81**, 259 (2025).

[39] G. Khaliullin and J. Chaloupka, Supporting data for manuscript "Orbital order and superconductivity in bilayer nickelate compounds" [Data set], Zenodo (2026), doi: 10.5281/zenodo.18155533.

[40] E. Pavarini, I. Dasgupta, T. Saha-Dasgupta, O. Jepsen, and O. K. Andersen, Band-structure trend in hole-doped cuprates and correlation with $T_{c\,\max}$, Phys. Rev. Lett. **87**, 047003 (2001).

[41] B. Y. Wang, Y. Zhong, S. Abadi, Y. Liu, Y. Yu, X. Zhang, Y.-M. Wu, R. Wang, J. Li, Y. Tarn, E. K. Ko, V. Thampy, M. Hashimoto, D. Lu, Y. S. Lee, T. P. Devereaux, C. Jia, H. Y. Hwang, and Z.-X. Shen, Electronic structure of compressively strained thin film $La_2PrNi_2O_7$, arXiv:2504.16372.

[42] W. Sun, Z. Jiang, B. Hao, S. Yan, H. Zhang, M. Wang, Y. Yang, H. Sun, Z. Liu, D. Ji, Z. Gu, J. Zhou, D. Shen, D. Feng, and Y. Nie, Observation of superconductivity-induced leading-edge gap in Sr-doped $La_3Ni_2O_7$ thin films, arXiv:2507.07409.